Protein quality control modulates the metabolic conservation in antibiotic tolerant *Campylobacter jejuni*

Jinsong Feng[1,2,3#], Shenmiao Li[4#], Yaxi Hu[1&], Martin Stahl[5], Lina Ma[1,2], Katelyn Knuff-Janzen[2], Kaidi Wang[4^], Marti Z. Hua[4], Bruce A. Vallance[5], Michael E. Konkel[6], B. Brett Finlay[2], Xiaonan Lu[1,4*]

[1] Food, Nutrition, and Health Program, Faculty of Land and Food Systems, The University of British Columbia, Vancouver, British Columbia, V6T 1Z4, Canada
[2] Michael Smith Laboratories, The University of British Columbia, Vancouver, British Columbia, V6T 1Z4, Canada
[3] Department of Food Science and Nutrition, Zhejiang University, Hangzhou, Zhejiang, 310058, China
[4] Department of Food Science and Agricultural Chemistry, Faculty of Agricultural and Environmental Sciences, McGill University, Sainte-Anne-de-Bellevue, Quebec, H9X 3V9, Canada
[5] British Columbia Children's Hospital Research Institute, Vancouver, British Columbia, V6H 3V4, Canada
[6] School of Molecular Biosciences, College of Veterinary Medicine, Washington State University, Pullman, WA 99164, USA

[#] Denoted as equal contribution
[*] Corresponding author. xiaonan.lu@mcgill.ca

[&] Current address: Food Science Program, Department of Chemistry, Carleton University, Ottawa, Ontario, K1S 5B6, Canada
[^] Current address: Department of Food and Bioproduct Sciences, University of Saskatchewan, Saskatoon, Saskatchewan, S7N 5A8, Canada

ABSTRACT

Antibiotic tolerance in bacteria emerges as a phenotypic variant known as persisters and has been implicated in recurrent bacterial infections. This tolerance manifests as suppressed metabolism. We demonstrate that *Campylobacter jejuni* readily forms persisters in response to both ampicillin and ciprofloxacin. Persisters induced by these two antibiotics with different mechanisms of actions experience consistent metabolic reprogramming, characterized by suppressed respiration and energy metabolism while conserving core metabolic processes. We reveal that the coordination of protein homeostasis underlies the metabolic reprogramming involved in persister formation. Mutating the caseinolytic protease gene *clpP*, a major component of the protein quality control system, compromises persister formation *in vitro* and impairs bacterial colonization in mouse. However, the deletion of *lon*, another component of the protein quality control system, or pre-activation of *clpP* by expressing artificial disordered protein fragments does not affect the antibiotic tolerance. This suggests that specific targets of ClpP rather than the entire quality control system are critical for persister formation. Our results reveal a convergent metabolic reprogramming in persisters, highlighting the potential to limit the emergence of antibiotic tolerance by counteracting adaptive metabolism elicited by antibiotic treatment.

Keywords: Persister, antibiotic tolerance, *Campylobacter*, metabolism

INTRODUCTION

Antibiotics are fundamental for treating bacterial infections across various medical disciplines. Beyond their clinical use, antibiotics also play a crucial role in other areas important to public health, such as food production and sanitation[1]. However, the effectiveness of antibiotics has been diminished, with the antibiotic failure has been largely attributed to the genetically-encoded antimicrobial resistance[1]. More recent studies indicated that many other factors significantly contribute to antibiotic failure, such as immunocompromised patients, biofilm-associated infections, and antibiotic persistence[2]. Within a population of antibiotic susceptible bacteria, certain subpopulation can survive under antibiotic treatment by acquiring transient tolerance, and the survived fractions are recognized as persister cells[3]. Persister cells are genetically identical to their antibiotic-susceptible counterparts and highly clinically relevant. This phenomenon is known to be present in various bacterial species and have evolved as a general environmental stress response in bacteria. An increasing number of studies have associated persisters with the recalcitrance and relapse of bacterial infections[4].

Campylobacter is the leading bacterial cause of human gastroenteritis worldwide. A recent clinical study reported a patient suffering from relapsing infections due to long-term *C. jejuni* colonization despite being prescribed antibiotics. Notably, this strain remained antibiotic sensitive[5]. Besides the transiently increased antibiotic tolerance, the presence of persisters has been linked to the emergence of antibiotic resistance in some studies when infections are treated with antibiotics[6]. In recent years, significant effort has been devoted to understanding the mechanisms behind persister formation. Persister cells were initially thought to be produced stochastically due to fluctuations in gene expression, but recent studies suggested that the formation of persisters could be genetically controlled and induced in response to antibiotics and environmental stresses. Numerous recent studies have demonstrated that bacterial persistence can be induced by different factors including carbon-source transition, starvation, oxidative stress, macrophage, DNA damage, pH, indole signalling, but not solely antibiotics[7]. Thus, this capability has likely evolved as a general environmental stress response rather than antibiotic tolerance alone.

In addition to slow growth and replication arrest, antibiotic tolerance has also been inherently linked to bacterial metabolism[8-9]. Bactericidal antibiotics, particularly gyrase inhibitors from the fluoroquinolone class, have been proposed to induce ATP bursts and subsequent oxidative damage under oxygen-rich conditions due to elevated production of reactive oxygen species (ROS) associated with increased aerobic respiratory activity[10]. Recent studies indicated that three major classes of bactericidal antibiotics promote the production of ROS, which play a critical role in most, if not all, killing process[11-13]. As ROS in bacteria are considered as toxic metabolic byproducts, their production is highly related to energy-consuming processes in bacteria[14]. Upon antibiotic exposure, stresses and damages in bacterial cells can initiate various energy-dependent biosynthesis processes, and certain metabolic activities might also increase to compensate for the loss of function of the antibiotic targets[14]. The surge in metabolism in bacterial cells results in the increased production and accumulation of ROS, exacerbating the cell damage, and this cycle continues until cell death. Therefore, bacteria exhibiting repressed metabolism show reduced production of ROS and increased tolerance of bactericidal antibiotic treatment[14]. In this ROS-lethality theory, interactions between antibiotics and their primary targets trigger stress and damage-mediated cellular processes and increased bacterial metabolism. This, in turn, causes oxidative damage and dysfunction of ROS-sensitive enzymes, contributing to cell death[14]. A more recent study indicated that antibiotic efficacy is strongly associated with bacterial metabolism, and combination of strong and weak metabolic dependent antibiotics can eliminate bacterial persisters more effectively[15]. However, inconsistent results were reported in another study, which showed that ofloxacin, a

bactericidal fluoroquinolone antibiotic primarily targeting on bacterial DNA gyrase, could achieve effective killing without excessive accumulation of intracellular ROS[16]. Several other studies also challenged the ROS-lethality theory, demonstrating that antibiotic treatment and the presence of ROS are independently linked to bacterial killing. These studies found no significant difference in the survival of bacteria grown aerobically or anaerobically when treated with antibiotics[17-18].

While the association between metabolic states and antibiotic tolerance is generally recognized, specific targets to either enhance or prevent persister formation have not been fully identified and remain under debate. Several studies have attributed antibiotic tolerance to the suppression of bacterial metabolism, including deficiencies in energy metabolism, arrested protein synthesis, and reduced activity of the respiratory and tricarboxylic acid (TCA) cycle[19-21]. However, in *Salmonella enteric* serovar Typhimurium, an ATP synthase deficient mutant (strain with *atp* operon deletion) with low levels of ATP production were shown to be more sensitive than wild-type to killing by ciprofloxacin[22]. Therefore, despite the increased studies and hypothesized mechanisms of antibiotic persistence, much of the molecular mechanisms underlying the increased antibiotic tolerance in persisters remains to be determined.

In the current study, our objective was to elucidate how downstream cellular processes related to antibiotic exposure and alterations in bacterial metabolism contribute to the development of tolerance to antibiotics that rely heavily on metabolic processes. We demonstrated that *C. jejuni* could develop tolerance to antibiotics with strong metabolic dependencies (*i.e.*, ampicillin and ciprofloxacin) concurrently with metabolic reprogramming. This reprogramming was facilitated by the regulatory activation of caseinolytic protease ClpP, which suppressed core metabolism. The metabolic suppression involved inhibiting ATP synthesis and redirecting carbon fluxes from the TCA cycle to the pentose phosphate pathway and S-adenosylmethionine cycle. Deleting *clpP* heightened sensitivity to oxidative stress, eliminated antibiotic tolerance, and reduced both *in vitro* and *in vivo* survival of *C. jejuni*. These findings unveiled a critical mechanism of antibiotic tolerance involving interactive metabolic reprogramming, orchestrated through *clpP*-mediated protein quality control. This understanding forms the foundation for developing additional robust strategies to combat bacterial antibiotic tolerance.

MATERIALS AND METHODS

Bacterial strains and growth conditions

C. jejuni strain F38011 is a representative clinical isolate obtained from a fecal sample from a human with bloody diarrhea, and was used in the current study[23]. Additionally, another three *C. jejuni* strains 81116, 87-95, and 11168 were used in antibiotic killing assay. The bacteria were routinely cultivated either on Mueller-Hinton agar (MHA) or in Mueller-Hinton broth (MHB) supplemented with selective antibiotics (chloramphenicol or kanamycin) at 37°C under microaerobic condition.

Construction of *C. jejuni* mutants and complementation

The mutants of *C. jejuni* F38011 were generated by replacing the genomic coding region of the targeted gene with a drug resistance gene using homologous recombination. The sequences of the primers are listed in **Table S1**. The *lon* deletion mutant was generated by homologous recombination and insertion of a chloramphenicol resistance cassette (Cm^R). The upstream and downstream regions flanking *lon* (lon^{up}, lon^{down}) were PCR-amplified using the primer pairs OLU182/OLU183 and OLU186/OLU187, respectively. The Cm^R gene was amplified from the plasmid pACYC184 using the primer pairs OLU184/OLU185. The above three PCR fragments were purified using the Gel/PCR purification kit

(Froggabio, CA) and inserted into EcoRI/XbaI-digested pUC19 using the NEBuilder® HiFi DNA Assembly Cloning Kit. The plasmid pUC19-*lon*^{up}-*Cm*^{R}-*lon*^{down} was introduced into *C. jejuni* strain F38011 via natural transformation. Transformants were selected on MHB supplemented with 2 µg/mL Cm (MHBCm2) and streaked on the MHBCm8 agar to confirm Cm resistance. Deletion of *lon* was confirmed by PCR.

The *clpP* deletion mutant of *C. jejuni* was generated using the similar protocol as described above. Briefly, upstream and downstream regions flanking *clpP* (*clpP*^{up}, *clpP*^{down}) were PCR-amplified using the primer pairs OUL196/OLU197 and OLU200/OLU201, respectively. The Cm^{R} gene was amplified from pACYC184 using the primer pair OLU198/OLU199. The engineered plasmid pUC19-*clpP*^{up}-*Cm*^{R}-*clpP*^{down} was transformed into *C. jejuni* strain F38011, followed by selection on the MHBCm2 and MHBCm8 agar, subsequently. Deletion of *clpP* was confirmed by PCR.

The complementary plasmids were derived from pRY107 (Kan resistance) vector (a gift from Dr. Konkel at Washington State University). The full *lon* gene including the coding region and ~500 bp upstream of the start codon was PCR-amplified using primers OLU228/OLU229. The PCR products were ligated with EcoRI/XbaI-digested pRY107 using the NEBuilder® HiFi DNA Assembly Cloning Kit. The complementary plasmid pRY107-*lon* was transformed into *C. jejuni ⊿lon* strain and the complementary transformants were selected on the MHBKan20 agar. To construct the complementary plasmid of *clpP*, the full *clpP* gene including the coding region and ~400 bp upstream of the start codon was PCR-amplified using the primers OLU230/231 and cloned into pRY107 subsequently. The complementary plasmid pRY107-*clpP* was transformed into *C. jejuni ⊿clpP* strain and the complementary transformants were selected on the MHBKan20 agar.

The *spoT* mutant of *C. jejuni* was generated using the similar technique above. Briefly, upstream and downstream regions flanking *spoT* (*spoT*^{up}, *spoT*^{down}) were PCR-amplified using the primer pairs *spoT*-FF/*spoT*-FR and *sopT*-RF/*sopT*-RR, respectively. The Kan^{R} gene was amplified from pUC18K2 using the primer pair *kan*-F/*kan*-R. The engineered plasmid pUC19-*spoT*^{up}-*Kan*^{R}-*spoT*^{down} was transformed into *C. jejuni* strain F38011, followed by selection on *kan* (50 µg/mL) agar, subsequently. Deletion of *spoT* was confirmed by PCR.

The *recA* deletion mutant of *C. jejuni* was generated using the similar protocol as described above. Briefly, upstream and downstream regions flanking *recA* (*recA*^{up}, *recA*^{down}) were PCR-amplified using the primer pairs *recA*-FF/*recA*-FR and *recA*-RF/*recA*-RR, respectively. The Cm^{R} gene was amplified from pRY111 using the primer pair *cm*-F/*cm*-R. The engineered plasmid pUC19-*recA*^{up}-Cm^{R}- *recA*^{down} was transformed into *C. jejuni* strain F38011, followed by selection on the MHBkan50 agar subsequently. Deletion of *recA* was confirmed by PCR.

Antibiotic killing and isolation of persister cells

Overnight *C. jejuni* culture was diluted to ~log 8 CFU/mL in MHB with specific antibiotic at final concentration: ampicillin 100 µg/mL or ciprofloxacin 1 µg/mL. The bacterial culture was kept with shaking at 37□ in a microaerobic condition. At indicated time points, aliquots of bacterial culture were collected, centrifuged, washed with PBS, and plated on MHA. After incubation for 24 hr, 10-100 colonies were enumerated for each data point unless further noted. Along with antibiotic exposure, development of a biphasic killing curve could confirm the formation of *C. jejuni* persister cells.

Determination of antibiotic MIC

Antibiotic MIC was determined using the micro-titration method. Overnight bacterial culture was diluted to ~log7 CFU/mL in MHB and added into 96-well flat-bottom clear polypropylene plates (Corning) with two-fold dilutions of antibiotic for a total volume of 100 µL. Plates were incubated at 37°C for 24 hr and then each absorbance at OD_{600} was measured using a Spectramax M3 microplate reader.

Lipid peroxidation

Lipid peroxidation of *C. jejuni* cells was determined using the BODIPY™581/591 C11 sensor kit (Invitrogen™) according to the manufacturer's instruction. Briefly, overnight *C. jejuni* F38011 wild-type and mutants were stained with dye in dark for 1 hr and then added to 96-well black microplates (~log 8 cells per well). Hydrogen peroxide (100 µM), ampicillin (100 µg/mL), and ciprofloxacin (1 µg/mL) treatment was separately conducted for 2 hr. Lipid peroxidation level was evaluated as the relative increase of fluorescence emission at 525 nm due to the treatment.

Determination of metabolism dependence

Metabolism dependence of *C. jejuni* persister cells was determined by supplementing 6-diazo-5-oxo-L-norleucine, glutamate, serine, aspartate, ferrous sulfate, or ferric chloride to the final concentration of 10 mM during antibiotic treatment. Metabolism dependence of persister cells were evaluated as variations on the survival rates after 4 hr of antibiotic treatment.

RNA-seq analysis

Total RNA of both untreated *C. jejuni* cells and persister cells were extracted using the RNeasy Mini Kit (Qiagen). Ribosomal RNA was removed by the RiboMinus Transcriptome Isolation Kit (Invitrogen) and mRNA was then purified using the RNeasy Mini Spin columns (Qiagen). The resulting transcriptome RNA was used for the construction of RNA-seq library using NEB Next mRNA Library Prep Reagent set from Illumina (NEB) according to the manufacturer's protocol. These constructed libraries were sequenced by Illumina HiSeq 2000 platform by paired-end chemistry. Sequence reads processing, mapping to *C. jejuni* NCTC 11168 genome (NC_002163), and quantification of differential expression (RPKM) were conducted using CLC genomic workbench. The functional annotation of genes was conducted in the Kyoto encyclopedia of genes and genomes (KEGG) database. Statistical significance is referred to as absolute log 2-fold change >1 and *p*-value <0.5.

Quantitative PCR analysis

C. jejuni cells were collected from both untreated group and treated group with exposure to antibiotics for 4 hr at which time most population entered the persistent state. RNA extraction was performed using the RNeasy mini kit (Qiagen) following the manufacturer's protocol. Total RNA concentration and purity were determined using a Nanodrop 2000 Spectrophotometer (Thermo Scientific). The cDNA was produced via SuperScript™ II Reverse Transcriptase (Invitrogen). The qPCR was performed using cDNA from bacterial samples with Power SYBR green PCR Master Mix (Applied Biosystems, Warrington, United Kingdom) on an ABI Prism 7000 Fast instrument (Life Technologies). The primers used for qPCR validation are listed in **Table S1**. Housekeeping genes *gyrA* and *rpoA* in *Campylobacter* were used as the internal controls. A total of 7 genes that were detected as differentially expressed in the RNA-seq results were selected as the targets for validation.

Label-free quantitative proteomics by LC-MS/MS

C. jejuni persister cells were collected and cell pellets were suspended in ammonium bicarbonate (100 mM) and lysed by bead beating on ice. The lysates were diluted and digested with trypsin. Digested peptides were desalted, and their concentration was determined by the bicinchoninic acid protein assay. The sample was then analyzed by LC-MS/MS using a Waters nanoACQUITY UPLC® system (Milford, United States) coupled with a Q Exactive HF hybrid quadrupole-Orbitrap mass spectrometer (Thermo Scientific, San Jose, United States). Raw mass spectrometry data were processed using the MaxQuant proteomics platform[24]. The false discovery rate was set at 0.01 at the peptide and protein levels. Proteins were identified with at least 2 peptides of a minimum length of 6 amino acids in Uniprot database using *C. jejuni* NTCT 11168 proteome (UP000031762). Protein relative abundance was quantified using the MaxQuant-LFQ algorithm[25]. The sample with a measured LFQ intensity in at least two out of the three samples was subjected to quantification. Statistical significance is referred to as absolute log 2-fold change>1 and *p*-value for two-tailed t-test <0.05.

COG category annotation

PSI-BLAST (version 2.2.31+) was used to categorize proteins of *C. jejuni* F38011 according to the COG database with default cut-off value[25]. Top PSI-BLAST hits were manually cured.

Metabolomics

Both untreated and persister cells were subjected to dual extraction for both hydrophilic metabolomics and hydrophobic lipidomics. Briefly, 10 μL of ^{13}C labeled hydrophilic metabolites and 10 μL of odd chain lipid molecules were added into bacterial samples as the internal standards. Then, 270 μL of ice-cold methanol (kept at -20°C) was added to quench cell metabolism. The metabolites of *C. jejuni* cells were released by three freeze-thaw cycles including flash freezing in liquid nitrogen for 1 min and sonication in ice water for 15 min. After adding 900 μL of methyl tert-butyl ether (MTBE), the samples were sonicated in ice water for 30 min to extract hydrophobic molecules. Next, the samples were mixed with 315 μL of cold H_2O and centrifuged at 20,817 ×*g* and 10°C for 2 min to achieve a clear phase separation between the hydrophilic methanol-H_2O layer (bottom) and the hydrophobic MTBE layer (top). The MTBE layer was collected, speed vacuum dried, reconstituted with 100 μL of isopropanol alcohol/acetonitrile (1:1, v/v), and stored at -80°C for further lipidomic analysis. The methanol-H_2O layer of the samples was kept at -20°C for 2 hr to precipitate the proteins. After centrifugation at 20,817 ×*g* and 4°C for 15 min, the supernatant was collected. This aqueous solution was dried in speed vacuum drier, reconstituted using 100 μL of acetonitrile/H_2O (1:1, v/v), and stored at -80°C for further metabolomic analysis. Quality control samples for both metabolomics and lipidomics were prepared by mixing 10 μL of each sample. One method-blank sample (*i.e.* an empty tube subjected to the overall extraction procedure) and two solvent-blank samples (*i.e.* reconstitution solvent) were prepared as the negative controls.

Metabolomic (positive and negative) and lipidomic (negative) analyses of the samples were conducted using an Agilent 1290 infinite UHPLC system (Agilent Technologies, Palo Alto, CA) coupled with a Bruker Impact II quadrupole-time-of-flight (QTOF) mass spectrometer (Bruker Daltonics, Bremen, Germany). For hydrophilic metabolomic analysis, samples were separated on a SeQuant ZIC-pHILIC column (2.1 × 150 mm, 3.5 μm, 100 Å). Mobile phase A contained 5 mM NH_4Ac in 95% H_2O and 5% acetonitrile and mobile phase B constituted of 5 mM NH_4Ac in 5% H_2O and 95% acetonitrile. The pH of mobile phase A was adjusted to 5 for positive mass spectral collection and the pH was maintained at 9.8 for negative mass spectral collection. Sample elution was achieved using a linear gradient at 30°C with a flow rate of 200 μL/min. Specifically, the gradient started with 95% B for the first 3 min, decreased to

75% B over 4 min, then to 25% B at 12 min, again to 5% B at 14 min, and finally maintained at 5% for 4 min. The column was then equilibrated at 95% B for 18 min before the injection of the next sample. Sample injection volume was optimized using quality control sample to maximize spectral intensity and avoid signal saturation.

For lipidomic negative analysis, samples were separated on a Waters Acquity UPLC BEH C_{18} column (1 × 100 mm, 1.7 μm, 130 Å). The mobile phases for the separation were A: 5 mM ammonium formate in acetonitrile/H_2O (6:4 v/v) and B: 5 mM ammonium formate in isopropanol alcohol/acetonitrile (9:1, v/v). The gradient sample elution program started with 5% B, increased to 40% B at 8 min, again to 70% B at 14 min, finally reached 95% B at 20 min, and maintained for 3 min. The column was then equilibrated at 5% B for 9 min before the next injection. The column was maintained at 25°C with a flow rate of 150 μL/min. Sample injection volume was optimized using the same approach as that for metabolomic analysis. An electrospray ionization source was used to ionize metabolites for MS detection and spectral information was recorded using the data-dependent MS/MS approach (auto MS/MS). The spectra for auto MS/MS were collected using a spectral rate of 8 Hz and *m/z* range of 50 to 1,200. For the auto MS/MS method, the MS/MS spectra were acquired using a stepping collision energy of 40 eV to 120 eV, an intensity threshold of 300, a cycle time of 3 s, a smart exclusion after two spectra, and a precursor reconsideration for intensity difference >1.8. The data-dependent LC-MS/MS results were normalized to total protein content according to the Bradford assay and processed using MS-DIAL (RIKEN, version 3.52). All the metabolic features with MS/MS spectra were manually confirmed using the MS-Finder (RIKEN, version 3.20), METLIN (Scripps Research), or an in-house metabolic library with an m/z tolerance of 5 ppm. Significantly regulated metabolic features were defined as absolute log 2-fold >2 and *p*-value for two-tailed t-test <0.05.

Gene set enrichment analysis

Gene set enrichment analysis (GSEA) was conducted using the Java (GSEA 3.0)-based graphical user interface with a pre-ranked list of the classic enrichment statistics[26-27]. GSEA involves determining whether a pre-defined set of genes/proteins is significantly different between the two groups, namely persister cells and untreated *C. jejuni* cells. The entire list of genes/proteins was ranked according to the expression difference in persister cells compared to that of untreated cells. The cumulative distribution function was constructed by performing 1000 random gene set membership assignments.

Visualization of the enrichment map

The significantly enriched terms in transcriptome and proteome analysis were visualized in Cytoscape 3.7.1[28]. Enrichment maps were built with stringent pathway similarity scores (Jaccard and overlap combined coefficient 0.6) and manually curated for the most representative groups of similar pathways and biological processes.

RESULTS

clpP is critical to achieve antibiotic tolerance of *C. jejuni*

Bacterial antibiotic persistence is often depicted by the biphasic killing curve, which unveils the presence of subpopulations that are killed at different rates under the same antibiotic treatment[7]. The amount of persisters within a bacterial population can vary, influenced by various genetic and environmental factors associated with different upstream and downstream events upon antibiotic treatment[29-31]. Although different classes of bactericidal antibiotics induce some common lethal events in cells, such as metabolic perturbations and accumulation of ROS, the interaction of antibiotics with their

primary targets can induce antibiotic-specific physiological changes and initiate different stress responses[32-34]. To evaluate the antibiotic tolerance of *C. jejuni* against two bactericidal antibiotics that interact with different primary targets, we used four representative *C. jejuni* strains with slightly varying genetic features. Through time-killing assays conducted with bactericidal concentrations of these antibiotics, we observed the heterogeneity within the *C. jejuni* population. Although most cells were susceptible and rapidly eliminated, a small fraction exhibited tolerance, manifesting a significantly slower killing rate (**Figure 1AB**). This biphasic killing pattern was consistent across all four tested strains. To avoid the possibility of transient modes of resistance leading to a slower killing rate, we repeated tolerance tests four times using the surviving bacterial population. No antibiotic resistance was detected as evidenced by the constant minimum inhibitory concentration (MIC) value (data not shown). Additionally, we ruled out the possibility of decreased killing rates due to antibiotic degradation over time by pre-incubating the antibiotics under the same conditions as the killing assay for 6 hr (data not shown). The MIC remained unchanged when the antibiotics were administered to *C. jejuni* strains. Therefore, the antibiotic tolerance observed in the subpopulation of *C. jejuni* was not a result of acquiring resistance mutations but rather a consequence of metabolism regulation.

The regulation of metabolic processes impacts the effectiveness of antibiotics that rely heavily on metabolic states[31]. Antibiotic-induced lesions can trigger bacterial stress responses, interfere with the toxin/antitoxin balance, and damage cell structures[12, 35-36]. The primary targets of ampicillin (*β*-lactams class) and ciprofloxacin (fluoroquinolone class) are penicillin-binding proteins and DNA topoisomerase II (DNA gyrase) and IV, respectively[34]. A previous study indicated that ampicillin at sub-MIC promotes amino acid depletion in *E. coli* and induces stringent responses[37], while ampicillin at concentrations above MIC interrupts peptidoglycan biosynthesis, resulting in altered proteostasis, membrane bulging, and cell lysis[38]. Ciprofloxacin binding to DNA gyrase and topoisomerase IV causes double-stranded breaks in DNA, trigging SOS responses. In addition to SOS responses, ciprofloxacin has been reported to induce cytoplasmic condensation and disrupt cellular homeostasis[16, 38]. In *C. jejuni*, *spoT* is associated with the stringent response and *recA* is associated with the SOS response[39-40], while *lon* and *clpP* encode ATP□dependent proteases crucial for intracellular proteolysis and protein quality control that are vital for maintaining protein homeostasis[41]. To characterize the molecular mechanisms underlying ampicillin and ciprofloxacin tolerance, we first assessed the survival of mutants deficient in the stringent response (Δ*spoT*), SOS response (Δ*recA*), and proteases (Δ*lon*, and Δ*clpP*) under antibiotic treatment (**Figure 1CD**). Deletion of *spoT* and *recA* did not affect the tolerance of *Campylobacter* to ampicillin. Compromised tolerance was observed only in the *recA* deletion mutant of *C. jejuni* when exposed to ciprofloxacin. Deletion of *lon* or *clpP* was expected to disrupt intracellular protein quality control and proteostasis. Surprisingly, mutations in *lon* and *clpP* had distinct effects on the antibiotic tolerance of *C. jejuni*. In bacteria, ClpP is considered a more selective protease that recognizes specific regions of substrates, whereas Lon is a more general protease that recognizes hydrophobic residues of substrates[42]. To confirm the role of *clpP* in ampicillin and ciprofloxacin tolerance, the antibiotic tolerance of *clpP* complemented mutant, Δ*clpP*::*clpP*, was assessed. Antibiotic tolerance of *C. jejuni* was reinstated by reintroducing the *clpP* gene into the *clpP* deletion mutant, confirming that the absence of *clpP* is responsible for the loss of antibiotic tolerance. Importantly, all these mutants exhibited similar MIC values compared to those of the wild-type strains and showed no significant growth defects (data not shown).

To further characterize this tolerant phenotype and elucidate the regulatory mechanisms underlying these tolerant cells, we performed the transcriptomic sequencing. Gene set enrichment analysis (GSEA)

conducted on the transcriptome of the antibiotic tolerance fraction of *C. jejuni* F38011 against two antibiotics with distinct mechanisms of actions revealed consistent regulatory patterns. These included the over-representation of pathways related to protein catabolism and quality control, SOS/stringent stress response, peptidoglycan synthesis, and RNA processing. Interestingly, the TCA cycle/respiration electron transport pathway was the sole under-represented pathway (**Figure 1F**). The reduced effectiveness of metabolic-dependent antibiotics, such as ampicillin (*β*-lactam class) and ciprofloxacin (quinolone class), has been linked to a decline in bacterial metabolic activity[31]. While bacterial metabolic activity typically correlates with growth and various biological processes, it can become uncoupled with growth and certain cellular process under specific conditions[31, 43]. Therefore, cellular processes that are commonly overrepresented in actively growing cells, particularly energy-dependent processes, could also be critical for persister cells that are in a metabolically suppressed state. Hence, we hypothesize that the pathways showing overrepresentation are crucial for antibiotic tolerance of *C. jejuni*. Using a genetic interaction network obtained from the STRING database (**Figure S2**), we identified *clpP* as the hub gene within the overrepresented pathways, validating the significance of these pathways. These findings collectively suggest that *clpP*-mediated protein quality control plays a pivotal role in the antibiotic tolerance phenotype of *C. jejuni* towards the tested antibiotics.

Regulatory events synchronized with *clpP* expression in *C. jejuni*

clpP plays a critical role in maintaining intracellular hemostasis, particularly proteostasis, by degrading misfolded proteins[44]. Recent studies have shown that disruption of *clpP* impairs proteostasis and re-sensitizes antibiotic-tolerant persister cells to strongly metabolism-dependent antibiotics[45-46]. In bacteria, ClpP functions as an ATP-dependent protease, recognizing and eliminating misfolded proteins. Moreover, certain antibiotics exert their effects by inducing protein mistranslation and peptidoglycan cross-linking[47]. Oxidative stress associated with the formation of ROS during antibiotic treatment can also lead to an increase in damaged and misfolded proteins[11, 48]. Therefore, we hypothesize that the expression of *clpP* would result in specific signatures on the proteome of antibiotic-tolerant *C. jejuni* cells, which exhibit a distinct metabolic state.

Transcriptomic and proteomic profiling were combined to characterize the metabolic changes of antibiotic-tolerant *C. jejuni* cells at both transcript and protein levels. GSEA on the proteome of *C. jejuni* cells confirmed the critical role of protein quality control in antibiotic tolerance, as evidenced by an overrepresented cluster. However, slight disparities were noted between the transcriptomic and proteomic profiles. The levels of differently expressed proteins and the abundance of the corresponding mRNA were not significantly correlated. Certain overrepresented pathways were exclusively identified at the transcriptomic level (**Figure 1F**). For example, while proteomic results highlighted the overrepresentation of ion transport-associated pathways in both antibiotic treatments, this phenomenon was observed only in ciprofloxacin-tolerant *C. jejuni* cells at the transcriptomic level. We also observed that ciprofloxacin induced more detectable pathway changes than ampicillin. Some consistent changes at both the transcript and protein levels were identified only in ciprofloxacin-treated *C. jejuni* cells, such as peptidoglycan synthesis, whereas ampicillin-treated *C. jejuni* cells showed overrepresentation of peptidoglycan synthesis only at the transcript level. Additionally, tRNA/rRNA processing was overrepresented at the transcript level but underrepresented at the protein level. Conversely, the protein folding-associated pathway was overrepresented in both antibiotic treatments, indicating significant changes under both conditions.

The combined analysis of transcriptomics and proteomics strongly suggests the significant involvement of protein quality control in the tolerance of *C. jejuni* cells to the applied antibiotics. GSEA on the proteome revealed a complex reorientation of protein regulation in antibiotic-tolerant *C. jejuni* cells rather than a general shutdown. Upon antibiotic exposure, the changes between transcriptomic and proteomic levels were not directly coupled, with some changes being antibiotic-specific. However, the consistent upregulation of the protein folding-associated pathway was well correlated at both the transcript and protein expression levels. This indicates that protein regulation and quality control are necessary in response to both ampicillin and ciprofloxacin treatments despite they are energy-consuming processes. In bacteria, Clp and Lon family proteases are estimated to carry out approximately 80% of cellular proteolysis[49-50]. Previous studies have highlighted the regulatory effects of ClpP-mediated protein quality control on various bacterial cellular processes, including cell growth, virulence, and stress response, achieved by targeting specific protein substrates[8, 51-52]. Moreover, our earlier findings demonstrated that the survival of *C. jejuni* under antibiotic treatments was significantly reduced only upon the deletion of *clpP*, not *lon*. This result aligns with the transcriptomic and proteomic profiling of the antibiotic-tolerant cells, which showed significant upregulation in the protein-folding pathway. This observation led us to hypothesize that *clpP* could serve as an effective focal point for uncovering active regulatory events.

To delve deeper into this hypothesis, we conducted a ClpP protein co-expression network analysis and identified 242 proteins strongly correlated with *clpP*, characterized by absolute Pearson correlation coefficients >0.8 and *p*-value <0.05 (**Table S2**). These proteins were predominately associated with pathways related to 1) energy production and conversion, 2) amino acid transport and metabolism, 3) translation, ribosomal structure, and biogenesis, 4) cell wall, membrane and envelope biogenesis, and 5) post-translational modification, protein turnover, and chaperones (**Figure 1E**). Antibiotic treatment can elevate the rate of translational errors, leading to disruptions in protein translation, accumulation of misfolded proteins, and the formation of protein aggregates[53-54]. A recent study observed a simultaneous occurrence of the emergence of antibiotic-tolerant bacterial cells and the development of protein aggregation[55]. Clp degradation complexes possess a two-component architecture with multiple active sites responsible for recognizing various substrates and hydrolyzing them into short peptides[56]. Within the Clp protease family, ClpP stands out as a barrel-shaped protease core with proteolytic sites, capable of interacting with other Clp family chaperones such as ClpA, ClpC, ClpE, and ClpX[56]. ClpP assembles with different chaperones through a range of assembly pathways to form distinct chaperone-protease complexes, each with distinct functions and activities. Therefore, proteins correlated with ClpP are believed to be actively involved in tagging, recognizing, and processing a wide range of substrates. Protein degradation by Clp proteases not only eliminates misfolded and damaged proteins but also targets short-lived regulatory proteins synthesized under stress conditions[57]. Thus, we hypothesize that to maintain proteostasis, ClpP-correlated proteins must be appropriately expressed, with their expression levels remaining relatively high even under conditions of metabolic suppression.

As anticipated, the relative expression of ClpP-correlated proteins was significantly higher than that of other proteins under both ampicillin and ciprofloxacin treatment (**Figure 2AB**). Protein synthesis is an energy-intensive process, with translation requiring approximately ten times more energy than transcription[58]. Regulatory mechanisms governing the proteome typically follow a cost-effective optimization model[9]. Bacteria react and adapt to environmental changes by reshaping their proteome, particularly by producing necessary products and energy while minimizing the protein burden[59]. Therefore, it is common to observe that the transcriptomic regulation does not always continue at the

proteome level due to yield-cost tradeoffs[60-61]. The transcript changes that subsequently reflect on the proteome highlight the necessity of redistributing resources to the upregulated pathways among different cellular processes. The conventional "structure-function paradigm" of proteins proposes that a stable conformational structure under certain physiological conditions is necessary for their functions. However, the more recent "disorder-function paradigm" reveals that the flexibility of the three-dimensional structure of proteins or certain regions of proteins endows them with functional promiscuity[62]. Studies have identified that the majority of the signaling and regulatory proteins are intrinsically disordered proteins (IDPs) or contain intrinsically disordered regions, enabling transient binding and interaction with specific enzymes and involvement in various post-translational modifications. Although IDPs in prokaryotes are generally less prevalent than in eukaryotes, bacteria are found to contain higher levels of IDPs than archaea. These IDPs contribute to the regulation of critical cellular processes, including stress responses, post-transcriptional processing, and cell division[63-65].

We then analyzed the disorder tendency of ClpP-correlated proteins using DFLpred[66] and categorized them into high, medium, and low disorder tendencies (**Table S3**). Surprisingly, proteins with a high disorder tendency exhibited the highest relative expression level within the ClpP-correlated protein cluster (**Figure 2CD**). Persister formation often involves stringent responses that downregulate genes encoding translational machinery and halt translation[67-68]. However, the synthesis of physiologically essential proteins is tightly controlled, maintaining consistency between transcription and translation[69]. Collective correlation analysis revealed a close dependency between the transcription and translation of high-disorder tendency proteins within the ClpP-correlated protein cluster (**Figure 2EF**). These findings highlighted the role of ClpP in regulating proteins with high disorder tendencies and its potential in regulating critical cellular processes. Based on these observations, high-disorder tendency proteins within the ClpP-correlated cluster were subject to strict regulation and likely play a critical role in the antibiotic tolerance of *C. jejuni*. These features were then mapped to KEGG metabolism pathways[70-71] and annotated with the corresponding regulatory patterns (**Figure 2G**). Pathways such as glycolysis or gluconeogenesis, the TCA cycle, oxidative phosphorylation, and amino acid metabolism were promoted to varying degrees, whereas only parts of fatty acid metabolism, biotin synthesis, oxidative phosphorylation, and histidine, lysine, and glutamate metabolism were suppressed.

Metabolic signatures of antibiotic tolerance in *C. jejuni*

Antibiotic persistence is a biological phenotype resulting from a series of complex regulatory events within bacterial cells. Therefore, systems-level approaches are necessary to map the information flow across the hierarchical control regimes of the cells, from RNA to molecular representations of cellular states[72]. Various omic approaches aligned with different stages of the cellular process as outlined in the "central dogma" provide complementary information. Previous studies have elucidated that bacterial antibiotic tolerance involves intricate regulation associated with metabolism, particularly in slow and non-proliferating states[11, 73]. Our findings expand on this knowledge by demonstrating that *C. jejuni* cells were not merely suppressed in core metabolism but were primed to respond to encountered stresses. To validate this suspected metabolic trajectory inferred from the transcriptomic and proteomic results, we conducted metabolomic analyses to observe changes in the abundance of the corresponding hydrophilic and hydrophobic metabolites (**Figure 3AD**, **Table S4**, and **Table S5**). The collective metabolomic data revealed a global decrease in the abundance of metabolites associated with core metabolism. Consistent with the observed regulatory patterns in biotin synthesis and the metabolism pathways of histidine, lysine and glutamate, the abundance of these metabolites was significantly downregulated (**Figure 3BC** and **Figure S3**). Importantly, key metabolites in glycolysis, the TCA cycle,

and amino acid metabolism were notably downregulated (**Figure 3BC** and **Figure S3**). However, the abundance of several key metabolites in nucleotide sugar metabolism and the pentose phosphate pathway, such as UDP-xylose, UDP-D-glucose, and UDP-glucuronate, significantly increased in response to both ampicillin and ciprofloxacin treatments. A previous study has demonstrated that sugar metabolism significantly influences bacterial persistence by affecting metabolic flux and proton motive force (PMF)[74]. The abundance of central carbon metabolites is closely linked to the TCA cycle and the electron transport chain, thereby influencing PMF[75]. PMF has been shown to affect the uptake of certain antibiotics by bacterial cells[76-78]. Supplementing central carbon metabolites at various glycolysis stages influences PMF at different levels and exhibits different potentiation effects with different antibiotics[75, 78-79]. Hence, we conclude that the core metabolism of antibiotic-tolerant *C. jejuni* is maintained in a suppressed state, while increased abundance of some metabolites indicates a key metabolic shift in the persister cells. Despite the proposed inhibition of fatty acid synthesis, our lipidomic analysis revealed an accumulation of fatty acids primarily with carbon chain lengths ranging from 14 to 18 (**Figure 3EF**). Conversely, the abundance of fatty acid synthesis co-factor biotin was significantly downregulated (**Figure S3**), suggesting that fatty acids accumulated through catabolism rather than anabolism.

Furthermore, the abundance of lysophospholipids (LPLs) with carbon chain lengths primarily of 16 and 18 was significantly upregulated in antibiotic-tolerant *C. jejuni* cells upon exposure to antibiotics (**Figure 3EF**). LPLs make up a small fraction (<1%) of the bacterial membrane composition and their accumulation is frequently observed in stressed bacteria[80]. These molecules can be generated through bacterial membrane degradation or phospholipid biosynthesis as metabolic intermediates[80]. The most common LPLs include lysophosphatidic acid, lysophosphatidylcholine, lysophosphatidylethanolamine, lysophosphatidylglycerol, lysophosphatidylinositol, and lysophosphatidylserine[80]. In response to stress, some pathogens activate phospholipase A1 encoded by the *pldA* gene to hydrolyze toxic oxidized phospholipids, producing LPLs and free fatty acids[81-82]. Accumulation of LPLs is considered a hallmark of lipid oxidation. A wide variety of LPLs were detected in *C. jejuni*, and the composition of these LPLs varied depending on environmental conditions. In particular, variations in oxygen levels can alter the composition of LPLs[83]. A previous study has shown that a high amount of LPLs is required for *C. jejuni* to maintain motility under oxygen-limited condition[83]. Although the specific role of LPLs and their related mechanisms in bacterial stress response remain unclear, they are known to contribute to membrane curvature stress and stability, thereby affecting membrane permeability[84-85]. Excessive generation of LPLs can lead to micellization of cell membrane and cause the formation of transient or steady pores[84]. Therefore, the generation of LPLs in bacteria must be tightly regulated. We identified a significant upregulation of *pldA* in antibiotic-tolerant *C. jejuni* cells (**Table S2**). Although no significant lipid peroxidation was induced by either ampicillin or ciprofloxacin (**Figure S4** and **Figure S5**), oxidized phosphatidylethanolamine intermediates were identified in antibiotic-tolerant *C. jejuni* cells (**Figure S6** and **Figure S7**), suggesting that antibiotic treatment induced lipid oxidation and the accumulation of oxidized LPLs. Oxidized LPLs are products of hydrolysis of oxidized phospholipids. As both proteostasis and membrane stability significantly contribute to homeostasis, deletion of *clpP* sensitized *C. jejuni* cells to oxidative stress by exacerbating membrane instability and affecting electron transport chain. Consistent with this, our results indicated that lipid peroxidation was elevated in the *clpP* deletion mutant.

To track the entire metabolic trajectory, we constructed a core metabolism map illustrating the direction of metabolic flux in *C. jejuni* (**Figure 4A**). This map provided additional insights not fully captured by transcriptomics and proteomics. As shown in **Figure 2G**, reactions involved in glycolysis and

gluconeogenesis exhibited an upregulated pattern. The metabolism map revealed that glycolytic flux was directed towards nucleotide sugar metabolism, while flux through glycolysis or gluconeogenesis might not be promoted. Antibiotic-tolerant *C. jejuni* cells displayed a shunted flow in the TCA cycle and an exhausted glutamate-glutamine cycle. Additionally, there was an increased flux towards the synthesis of redox-associated metabolites, such as S-adenosylmethionine, riboflavin-5-phosphate, and menaquinone-6, indicating redox-driven metabolic signatures.

Pathogenicity relevance of antibiotic tolerance capacity

The above results have underscored the association between antibiotic tolerance and level of LPLs. Additionally, our metabolomic results revealed that the deletion of *clpP* not only compromised antibiotic tolerance but also exacerbated redox-associated lipid peroxidation. A study showed that lysophosphatidylethanolamine might contribute to *C. jejuni* virulence, demonstrating toxicity to epithelial cells (human HeLa and Caco-2 cells) and causing hemolysis of red blood cells[86]. Therefore, oxidative stress induced during pathogen-host interactions and immune reactions can stimulate the generation of lysophosphatidylethanolamine, resulting in the expression of *C. jejuni* virulence. This may explain why *C. jejuni* can invade the epithelial barrier and cause bloody diarrhea despite lacking common virulence factors such as type III secretion system[86-87]. However, lipid oxidation and the formation of LPLs can be both beneficial and disruptive for bacteria during host-microbe interactions as they affect membrane stability and cellular homeostasis. We then evaluated whether the disruption of antibiotic tolerance via compromised *clpP* affected the *in vivo* survival of *C. jejuni*, given that the antimicrobial response of macrophage is primarily mediated by elevated redox levels[88]. To determine the pathogenic relevance associated with antibiotic tolerance, we initially compared the survival of the wild-type and *clpP* mutant strains in RAW 264.7 macrophages. Both strains exhibited similar adherence levels, approximately 6 CFU/mL at 3 hr post-infection. However, the *clpP* mutant lost its ability to survive within macrophages, becoming undetectable after 8 hr post-infection. The loss of survival observed in the *clpP* mutant may be attributed to dysfunction in redox homeostasis.

To further validate this mechanism, we used mice deficient in the single IgG IL-1-related receptor (*sigirr*) to assess *C. jejuni* infection. *SIGIRR* is responsible for activating innate immunity to produce antimicrobial radicals. Deletion of *sigirr* would impair colonization resistance in mice due to the disfunction of radical production[89]. We used a reference strain, *C. jejuni* 81-176, to assess the colonization capacity of *C. jejuni* F38011. Both wild-type strains exhibited similar peak colonization at 7 days post-infection, with bacterial loads of ~8 CFU/g feces (**Figure 4C**). Although the *clpP*-deficient mutant could colonize the cecum in *sigirr*-/- mice, the colonization load was significantly lower than that of its wild-type counterpart. Upon examining the localization of *C. jejuni* within *sigirr*-/- tissues, we observed that clumpy wild-type cells adhered to the intestinal epithelium but were absent within the crypts (**Figure 4D**). By co-staining *C. jejuni* antigens along with *β*-actin, we observed that *C. jejuni* F38011 wild-type cells were repelled by the cytoskeleton of the epithelial cells, remaining only on the surface of the epithelial layer. In contrast, the *clpP* mutant was not clearly observed on the surface of the epithelial layer, suggesting that even impaired innate immunity could eradicate the *clpP* mutant (**Figure 4E**). These results collectively demonstrated a clear correlation between pathogenicity and antibiotic tolerance in *C. jejuni*, primarily driven by the function of ClpP.

DISCUSSION

Antibiotic persistence was initially perceived as a series of stochastic events[7]. However, recent studies have unveiled numerous distinct regulatory mechanisms involved in achieving bacterial antibiotic

persistence[8, 55, 58]. The persistence-related genetic loci include but not limit to genes encoding toxin-antitoxin modules, (p)ppGpp synthetase I SpoT/RelA, and protease Lon[90]. Although there is a consensus on the association between low metabolism and antibiotic persistence, the full extent of this dependency remains to be fully investigated[8-9, 55]. Previous studies have demonstrated the effectiveness of antimicrobials targeting *clpP* in eradicating antibiotic-tolerant persister cells[45-46]. Consistent with these findings, our current study suggests that the antibiotic persistence of *C. jejuni* is dependent on metabolic regulations. Although a broad array of metabolic pathways could be implicated in antibiotic persistence, multi-omics analysis identified protein quality control as a significantly enriched pathway from both transcriptomic and proteomic perspectives. Further supporting this, antibiotic killing assays showed that the deletion of *clpP* compromised bacterial antibiotic persistence. ClpP is a major protein quality control protease in bacteria utilizing ATP to remove damaged and misfolded proteins[91]. Under certain conditions, it is also responsible for the regulated degradation of regulatory proteins[8, 92]. Other ATP-dependent proteases, such as Lon, HslUV, and FtsH, also play critical roles in protein quality control, similar to ClpP-mediated processes[91]. However, the association between antibiotic persistence and protein quality control has so far been specifically identified and validated only for ClpP.

Previous studies have reported distinct substrates of ClpP in different physiological states, indicating its potential regulatory functions in maintaining the proteostasis of selected proteins[8, 51-52]. Mutation of *clpP* has been implicated not only in protein folding but also in metabolism. Recent studies have shown that *clpP* mutation disrupts central carbon metabolism, energy metabolism, and co-factor synthesis pathways[93]. A more comprehensive understanding of the cellular pathways associated with the activation of *clpP* could help decipher the mechanism of bacterial antibiotic tolerance. However, it remains unclear how *clpP* deletion triggers metabolic repression and antibiotic tolerance, and under what biological contexts these effects can be observed. One of the most significant findings of our study is the link between ClpP and lipid oxidation and LPLs, which has not been previously reported. Previous studies have indicated that the TCA cycle and central carbon metabolites significantly affect antibiotic persistence, with effects varying depending on species and environmental conditions. This underscores the dependency of antibiotic persistence on central carbon metabolism, where intermediates vary based on pathway alterations. In *Campylobacter*, the highly branched respiratory enables the utilization of diverse electron donors and acceptors[94].

Modulation of intracellular redox has been recognized to influence antibiotic susceptibility[96-97]. Previous studies have demonstrated that bactericidal antibiotics can trigger the generation of reactive oxygen species *in vitro*, particularly in the presence of elevated levels of transition metals[98]. An *in vivo* study found that bactericidal antibiotics induce the formation of hydroxyl radicals[11]. Hence, the stability of redox-related proteins is vital for bacterial survival during antibiotic treatment. For example, a mutation in respiratory complex I identified during *in vitro* evolution of *E. coli* resulted in cytoplasm desensitization to oxidation and increased antibiotic tolerance[99]. Antibiotic treatment is also believed to induce changes in intracellular redox levels, activating cellular stress mechanisms and contributing to antibiotic-induced cell death[100-101]. In our current study, we revealed an additional association between redox dynamics and antibiotic efficacy, showing that *clpP* deletion leads to increased sensitivity, particularly under oxidative conditions. Given the role of ClpP in maintaining the expression of physiologically essential proteins, we identified relevant proteins through co-expression networks. Our findings show that antibiotic tolerance mediated by ClpP is dependent on redox, as evidenced by the accumulation of lysophosphatidylethanolamine and oxidized phosphatidylethanolamine (**Figure S8**). Deletion of *clpP* may result in improper translation of redox-maintaining proteins, as indicated by the

accumulation of anabolic lipid peroxidation under oxidative conditions (**Figure S4** and **Figure S5**). This funding suggests that the level of lysophosphatidylethanolamine, a novel virulence factor recently identified in *C. jejuni*[86], is also related to ClpP. A previous study proposed that *C. jejuni* mutants unable to produce lysophosphatidylethanolamine exhibit low cytotoxicity[94]. Additionally, our results suggested that dysfunction of ClpP can lead to excessive accumulation of LPLs, affecting the colonization and cytotoxicity of *C. jejuni* both *in vitro* and *vivo*. Overall, our study observed consistent persistence dependent on metabolism in *C. jejuni* treated with antibiotics with different mechanisms of actions. While persistence is typically associated with a low metabolic state, persistence-conferring reprogramming of metabolism in certain pathways actively contributes to the survival of bacterial persisters.

In conclusion, as we strive to eradicate bacterial antibiotic persistence, targeting the associated metabolic reprogramming presents a promising strategy[14, 102]. This study demonstrated that disrupting or constraining critical pathways related to proteostasis and oxidative stress can limit the ability of bacteria to withstand antibiotics, with ClpP identified as one of the critical targets. The disruption of this protease, which is vital for *C. jejuni* to maintain proteostasis and homeostasis, significantly reduced the survival of *C. jejuni* both *in vitro* and in *vivo*. We have uncovered comprehensive metabolic reprogramming events that can inform the development of counter or synergic strategies to inactivate antibiotic-tolerant *C. jejuni* persister cells. Our findings shed light on the metabolic landscape of antibiotic persistence and propose potential solutions to control this challenging and heterogeneous bacterial population.

ACKNOWLEDGEMENT

This work was supported by funds given to X.L. from the Natural Sciences and Engineering Research Council of Canada (NSERC RGPIN-2019-03960, NSERC RGPIN-2019-00024), from Genome Canada and Genome British Columbia (SIP021), and from the Genomics Integration Program of Genome Quebec.

REFERENCES

1. Cook, M. A.; Wright, G. D., The past, present, and future of antibiotics. *Science Translational Medicine* **2022,** *14* (657), eabo7793.
2. de la Fuente-Nunez, C.; Cesaro, A.; Hancock, R. E., Antibiotic failure: Beyond antimicrobial resistance. *Drug Resistance Updates* **2023**, 101012.
3. Lewis, K., Persister cells. *Annual review of microbiology* **2010,** *64*, 357-372.
4. Fisher, R. A.; Gollan, B.; Helaine, S., Persistent bacterial infections and persister cells. *Nature Reviews Microbiology* **2017,** *15* (8), 453-464.
5. Bloomfield, S. J.; Midwinter, A. C.; Biggs, P. J.; French, N. P.; Marshall, J. C.; Hayman, D. T.; Carter, P. E.; Thornley, C.; Yap, R.; Benschop, J., Long-term colonization by Campylobacter jejuni within a human host: evolution, antimicrobial resistance, and adaptation. *The Journal of Infectious Diseases* **2018,** *217* (1), 103-111.
6. Windels, E. M.; Michiels, J. E.; Fauvart, M.; Wenseleers, T.; Van den Bergh, B.; Michiels, J., Bacterial persistence promotes the evolution of antibiotic resistance by increasing survival and mutation rates. *The ISME journal* **2019,** *13* (5), 1239-1251.
7. Balaban, N. Q.; Helaine, S.; Lewis, K.; Ackermann, M.; Aldridge, B.; Andersson, D. I.; Brynildsen, M. P.; Bumann, D.; Camilli, A.; Collins, J. J., Definitions and guidelines for research on antibiotic persistence. *Nature Reviews Microbiology* **2019,** *17* (7), 441-448.
8. Michel, A.; Agerer, F.; Hauck, C. R.; Herrmann, M.; Ullrich, J.; Hacker, J.; Ohlsen, K., Global regulatory impact of ClpP protease of Staphylococcus aureus on regulons involved in virulence, oxidative stress response, autolysis, and DNA repair. *Journal of bacteriology* **2006,** *188* (16), 5783-5796.
9. Dekel, E.; Alon, U., Optimality and evolutionary tuning of the expression level of a protein. *Nature* **2005,** *436* (7050), 588.
10. Dwyer, D. J.; Kohanski, M. A.; Hayete, B.; Collins, J. J., Gyrase inhibitors induce an oxidative damage cellular death pathway in Escherichia coli. *Molecular systems biology* **2007,** *3* (1), 91.
11. Kohanski, M. A.; Dwyer, D. J.; Hayete, B.; Lawrence, C. A.; Collins, J. J., A common mechanism of cellular death induced by bactericidal antibiotics. *Cell* **2007,** *130* (5), 797-810.
12. Kohanski, M. A.; Dwyer, D. J.; Wierzbowski, J.; Cottarel, G.; Collins, J. J., Mistranslation of membrane proteins and two-component system activation trigger antibiotic-mediated cell death. *Cell* **2008,** *135* (4), 679-690.
13. Foti, J. J.; Devadoss, B.; Winkler, J. A.; Collins, J. J.; Walker, G. C., Oxidation of the guanine nucleotide pool underlies cell death by bactericidal antibiotics. *Science* **2012,** *336* (6079), 315-319.
14. Stokes, J. M.; Lopatkin, A. J.; Lobritz, M. A.; Collins, J. J., Bacterial metabolism and antibiotic efficacy. *Cell metabolism* **2019,** *30* (2), 251-259.
15. Zheng, E. J.; Stokes, J. M.; Collins, J. J., Eradicating bacterial persisters with combinations of strongly and weakly metabolism-dependent antibiotics. *Cell chemical biology* **2020,** *27* (12), 1544-1552. e3.
16. Cayron, J.; Oms, T.; Schlechtweg, T.; Zedek, S.; Van Melderen, L., TisB protein is the single molecular determinant underlying multiple downstream effects of ofloxacin in Escherichia coli. *Science Advances* **2024,** *10* (13), eadk1577.
17. Liu, Y.; Imlay, J. A., Cell death from antibiotics without the involvement of reactive oxygen species. *Science* **2013,** *339* (6124), 1210-1213.
18. Keren, I.; Wu, Y.; Inocencio, J.; Mulcahy, L. R.; Lewis, K., Killing by bactericidal antibiotics does not depend on reactive oxygen species. *Science* **2013,** *339* (6124), 1213-1216.
19. Kwan, B. W.; Valenta, J. A.; Benedik, M. J.; Wood, T. K., Arrested protein synthesis increases persister-like cell formation. *Antimicrobial agents and chemotherapy* **2013,** *57* (3), 1468-1473.

20. Manuse, S.; Shan, Y.; Canas-Duarte, S. J.; Bakshi, S.; Sun, W.-S.; Mori, H.; Paulsson, J.; Lewis, K., Bacterial persisters are a stochastically formed subpopulation of low-energy cells. *PLoS biology* **2021,** *19* (4), e3001194.
21. Prax, M.; Bertram, R., Metabolic aspects of bacterial persisters. *Frontiers in cellular and infection microbiology* **2014,** *4*, 148.
22. Braetz, S.; Schwerk, P.; Thompson, A.; Tedin, K.; Fulde, M., Salmonella central carbon metabolism enhances bactericidal killing by fluoroquinolone antibiotics. *Antimicrobial Agents and Chemotherapy* **2022,** *66* (7), e02344-21.
23. Konkel, M. E.; Christensen, J. E.; Dhillon, A. S.; Lane, A. B.; Hare-Sanford, R.; Schaberg, D. M.; Larson, C. L., Campylobacter jejuni strains compete for colonization in broiler chicks. *Applied and environmental microbiology* **2007,** *73* (7), 2297-2305.
24. Cox, J.; Hein, M. Y.; Luber, C. A.; Paron, I.; Nagaraj, N.; Mann, M., Accurate proteome-wide label-free quantification by delayed normalization and maximal peptide ratio extraction, termed MaxLFQ. *Molecular & cellular proteomics* **2014,** *13* (9), 2513-2526.
25. Galperin, M. Y.; Makarova, K. S.; Wolf, Y. I.; Koonin, E. V., Expanded microbial genome coverage and improved protein family annotation in the COG database. *Nucleic acids research* **2015,** *43* (D1), D261-D269.
26. Reimand, J.; Isserlin, R.; Voisin, V.; Kucera, M.; Tannus-Lopes, C.; Rostamianfar, A.; Wadi, L.; Meyer, M.; Wong, J.; Xu, C., Pathway enrichment analysis and visualization of omics data using g: Profiler, GSEA, Cytoscape and EnrichmentMap. *Nature protocols* **2019,** *14* (2), 482-517.
27. Subramanian, A.; Tamayo, P.; Mootha, V. K.; Mukherjee, S.; Ebert, B. L.; Gillette, M. A.; Paulovich, A.; Pomeroy, S. L.; Golub, T. R.; Lander, E. S., Gene set enrichment analysis: a knowledge-based approach for interpreting genome-wide expression profiles. *Proceedings of the National Academy of Sciences* **2005,** *102* (43), 15545-15550.
28. Cline, M. S.; Smoot, M.; Cerami, E.; Kuchinsky, A.; Landys, N.; Workman, C.; Christmas, R.; Avila-Campilo, I.; Creech, M.; Gross, B., Integration of biological networks and gene expression data using Cytoscape. *Nature protocols* **2007,** *2* (10), 2366.
29. Lechner, S.; Lewis, K.; Bertram, R., Staphylococcus aureus persisters tolerant to bactericidal antibiotics. *Microbial Physiology* **2012,** *22* (4), 235-244.
30. Vega, N. M.; Allison, K. R.; Khalil, A. S.; Collins, J. J., Signaling-mediated bacterial persister formation. *Nature chemical biology* **2012,** *8* (5), 431-433.
31. Lopatkin, A. J.; Stokes, J. M.; Zheng, E. J.; Yang, J. H.; Takahashi, M. K.; You, L.; Collins, J. J., Bacterial metabolic state more accurately predicts antibiotic lethality than growth rate. *Nature microbiology* **2019,** *4* (12), 2109-2117.
32. Kohanski, M. A.; Dwyer, D. J.; Collins, J. J., How antibiotics kill bacteria: from targets to networks. *Nature Reviews Microbiology* **2010,** *8* (6), 423-435.
33. Gutierrez, A.; Stokes, J. M.; Matic, I., Our evolving understanding of the mechanism of quinolones. *Antibiotics* **2018,** *7* (2), 32.
34. Darby, E. M.; Trampari, E.; Siasat, P.; Gaya, M. S.; Alav, I.; Webber, M. A.; Blair, J. M., Molecular mechanisms of antibiotic resistance revisited. *Nature Reviews Microbiology* **2023,** *21* (5), 280-295.
35. Maisonneuve, E.; Gerdes, K., Molecular mechanisms underlying bacterial persisters. *Cell* **2014,** *157* (3), 539-548.
36. Brauner, A.; Fridman, O.; Gefen, O.; Balaban, N. Q., Distinguishing between resistance, tolerance and persistence to antibiotic treatment. *Nature Reviews Microbiology* **2016,** *14* (5), 320-330.

37. Mathieu, A.; Fleurier, S.; Frenoy, A.; Dairou, J.; Bredeche, M.-F.; Sanchez-Vizuete, P.; Song, X.; Matic, I., Discovery and function of a general core hormetic stress response in E. coli induced by sublethal concentrations of antibiotics. *Cell reports* **2016,** *17* (1), 46-57.
38. Wong, F.; Stokes, J. M.; Cervantes, B.; Penkov, S.; Friedrichs, J.; Renner, L. D.; Collins, J. J., Cytoplasmic condensation induced by membrane damage is associated with antibiotic lethality. *Nature communications* **2021,** *12* (1), 2321.
39. Gaasbeek, E. J.; van der Wal, F. J.; van Putten, J. P.; de Boer, P.; van der Graaf-van Bloois, L.; de Boer, A. G.; Vermaning, B. J.; Wagenaar, J. A., Functional characterization of excision repair and RecA-dependent recombinational DNA repair in Campylobacter jejuni. *Journal of bacteriology* **2009,** *191* (12), 3785-3793.
40. Gaynor, E. C.; Wells, D. H.; MacKichan, J. K.; Falkow, S., The Campylobacter jejuni stringent response controls specific stress survival and virulence□associated phenotypes. *Molecular microbiology* **2005,** *56* (1), 8-27.
41. Bittner, L. M.; Arends, J.; Narberhaus, F., Mini review: ATP□dependent proteases in bacteria. *Biopolymers* **2016,** *105* (8), 505-517.
42. Mahmoud, S. A.; Chien, P., Regulated proteolysis in bacteria. *Annual review of biochemistry* **2018,** *87* (1), 677-696.
43. Pu, Y.; Zhao, Z.; Li, Y.; Zou, J.; Ma, Q.; Zhao, Y.; Ke, Y.; Zhu, Y.; Chen, H.; Baker, M. A., Enhanced efflux activity facilitates drug tolerance in dormant bacterial cells. *Molecular cell* **2016,** *62* (2), 284-294.
44. Kirstein, J.; Molière, N.; Dougan, D. A.; Turgay, K., Adapting the machine: adaptor proteins for Hsp100/Clp and AAA+ proteases. *Nature Reviews Microbiology* **2009,** *7* (8), 589.
45. Kirstein, J.; Hoffmann, A.; Lilie, H.; Schmidt, R.; Rübsamen□Waigmann, H.; Brötz□Oesterhelt, H.; Mogk, A.; Turgay, K., The antibiotic ADEP reprogrammes ClpP, switching it from a regulated to an uncontrolled protease. *EMBO molecular medicine* **2009,** *1* (1), 37-49.
46. Conlon, B. P.; Nakayasu, E. S.; Fleck, L. E.; LaFleur, M. D.; Isabella, V. M.; Coleman, K.; Leonard, S. N.; Smith, R. D.; Adkins, J. N.; Lewis, K., Activated ClpP kills persisters and eradicates a chronic biofilm infection. *Nature* **2013,** *503* (7476), 365-370.
47. Nguyen, D.; Joshi-Datar, A.; Lepine, F.; Bauerle, E.; Olakanmi, O.; Beer, K.; McKay, G.; Siehnel, R.; Schafhauser, J.; Wang, Y., Active starvation responses mediate antibiotic tolerance in biofilms and nutrient-limited bacteria. *Science* **2011,** *334* (6058), 982-986.
48. Belenky, P.; Jonathan, D. Y.; Porter, C. B.; Cohen, N. R.; Lobritz, M. A.; Ferrante, T.; Jain, S.; Korry, B. J.; Schwarz, E. G.; Walker, G. C., Bactericidal antibiotics induce toxic metabolic perturbations that lead to cellular damage. *Cell reports* **2015,** *13* (5), 968-980.
49. Maurizi, M. R.; Thompson, M. W.; Singh, S. K.; Kim, S.-H., [23] Endopeptidase Clp: ATP-dependent Clp protease from Escherichia coli. In *Methods in enzymology*, Elsevier: 1994; Vol. 244, pp 314-331.
50. Goldberg, A. L.; Moerschell, R. P.; Hachung, C.; Maurizi, M. R., [25] ATP-dependent protease La (Lon) from Escherichia coli. In *Methods in enzymology*, Elsevier: 1994; Vol. 244, pp 350-375.
51. Sass, P.; Josten, M.; Famulla, K.; Schiffer, G.; Sahl, H.-G.; Hamoen, L.; Brötz-Oesterhelt, H., Antibiotic acyldepsipeptides activate ClpP peptidase to degrade the cell division protein FtsZ. *Proceedings of the National Academy of Sciences* **2011,** *108* (42), 17474-17479.
52. Gaillot, O.; Pellegrini, E.; Bregenholt, S.; Nair, S.; Berche, P., The ClpP serine protease is essential for the intracellular parasitism and virulence of Listeria monocytogenes. *Molecular microbiology* **2000,** *35* (6), 1286-1294.

53. Carter, A. P.; Clemons, W. M.; Brodersen, D. E.; Morgan-Warren, R. J.; Wimberly, B. T.; Ramakrishnan, V., Functional insights from the structure of the 30S ribosomal subunit and its interactions with antibiotics. *Nature* **2000,** *407* (6802), 340.
54. Ling, J.; Cho, C.; Guo, L.-T.; Aerni, H. R.; Rinehart, J.; Söll, D., Protein aggregation caused by aminoglycoside action is prevented by a hydrogen peroxide scavenger. *Molecular cell* **2012,** *48* (5), 713-722.
55. Pu, Y.; Li, Y.; Jin, X.; Tian, T.; Ma, Q.; Zhao, Z.; Lin, S.-y.; Chen, Z.; Li, B.; Yao, G., ATP-dependent dynamic protein aggregation regulates bacterial dormancy depth critical for antibiotic tolerance. *Molecular cell* **2019,** *73* (1), 143-156. e4.
56. Kress, W.; Maglica, Ž.; Weber-Ban, E., Clp chaperone–proteases: structure and function. *Research in microbiology* **2009,** *160* (9), 618-628.
57. Frees, D.; Qazi, S. N.; Hill, P. J.; Ingmer, H., Alternative roles of ClpX and ClpP in Staphylococcus aureus stress tolerance and virulence. *Molecular microbiology* **2003,** *48* (6), 1565-1578.
58. Warner, J. R., The economics of ribosome biosynthesis in yeast. *Trends in biochemical sciences* **1999,** *24* (11), 437-440.
59. Mori, M.; Marinari, E.; De Martino, A., A yield-cost tradeoff governs Escherichia coli's decision between fermentation and respiration in carbon-limited growth. *NPJ systems biology and applications* **2019,** *5* (1), 16.
60. Jensen, P. A.; Zhu, Z.; van Opijnen, T., Antibiotics disrupt coordination between transcriptional and phenotypic stress responses in pathogenic bacteria. *Cell reports* **2017,** *20* (7), 1705-1716.
61. Liu, Y.; Beyer, A.; Aebersold, R., On the dependency of cellular protein levels on mRNA abundance. *Cell* **2016,** *165* (3), 535-550.
62. Trivedi, R.; Nagarajaram, H. A., Intrinsically disordered proteins: An overview. *International journal of molecular sciences* **2022,** *23* (22), 14050.
63. Cohan, M. C.; Pappu, R. V., Making the case for disordered proteins and biomolecular condensates in bacteria. *Trends in Biochemical Sciences* **2020,** *45* (8), 668-680.
64. Dunker, A. K.; Lawson, J. D.; Brown, C. J.; Williams, R. M.; Romero, P.; Oh, J. S.; Oldfield, C. J.; Campen, A. M.; Ratliff, C. M.; Hipps, K. W., Intrinsically disordered protein. *Journal of molecular graphics and modelling* **2001,** *19* (1), 26-59.
65. Pavlović-Lažetić, G. M.; Mitić, N. S.; Kovačević, J. J.; Obradović, Z.; Malkov, S. N.; Beljanski, M. V., Bioinformatics analysis of disordered proteins in prokaryotes. *BMC bioinformatics* **2011,** *12*, 1-22.
66. Meng, F.; Kurgan, L., DFLpred: High-throughput prediction of disordered flexible linker regions in protein sequences. *Bioinformatics* **2016,** *32* (12), i341-i350.
67. Boutte, C. C.; Crosson, S., Bacterial lifestyle shapes stringent response activation. *Trends in microbiology* **2013,** *21* (4), 174-180.
68. Reiß, S.; Pané-Farré, J.; Fuchs, S.; François, P.; Liebeke, M.; Schrenzel, J.; Lindequist, U.; Lalk, M.; Wolz, C.; Hecker, M., Global analysis of the Staphylococcus aureus response to mupirocin. *Antimicrobial agents and chemotherapy* **2012,** *56* (2), 787-804.
69. Marguerat, S.; Schmidt, A.; Codlin, S.; Chen, W.; Aebersold, R.; Bähler, J., Quantitative analysis of fission yeast transcriptomes and proteomes in proliferating and quiescent cells. *Cell* **2012,** *151* (3), 671-683.
70. Kanehisa, M.; Goto, S.; Sato, Y.; Kawashima, M.; Furumichi, M.; Tanabe, M., Data, information, knowledge and principle: back to metabolism in KEGG. *Nucleic acids research* **2013,** *42* (D1), D199-D205.
71. Darzi, Y.; Letunic, I.; Bork, P.; Yamada, T., iPath3. 0: interactive pathways explorer v3. *Nucleic acids research* **2018,** *46* (W1), W510-W513.

72. Horgan, R. P.; Kenny, L. C., 'Omic'technologies: genomics, transcriptomics, proteomics and metabolomics. *Obstetrician & Gynaecologist* **2011,** *13* (3).
73. Lewis, K., Persister cells, dormancy and infectious disease. *Nature Reviews Microbiology* **2007,** *5* (1), 48-56.
74. Cabral, D. J.; Wurster, J. I.; Belenky, P., Antibiotic persistence as a metabolic adaptation: stress, metabolism, the host, and new directions. *Pharmaceuticals* **2018,** *11* (1), 14.
75. Meylan, S.; Porter, C. B.; Yang, J. H.; Belenky, P.; Gutierrez, A.; Lobritz, M. A.; Park, J.; Kim, S. H.; Moskowitz, S. M.; Collins, J. J., Carbon sources tune antibiotic susceptibility in Pseudomonas aeruginosa via tricarboxylic acid cycle control. *Cell chemical biology* **2017,** *24* (2), 195-206.
76. Farha, M. A.; French, S.; Stokes, J. M.; Brown, E. D., Bicarbonate alters bacterial susceptibility to antibiotics by targeting the proton motive force. *ACS infectious diseases* **2017,** *4* (3), 382-390.
77. Radlinski, L. C.; Rowe, S. E.; Brzozowski, R.; Wilkinson, A. D.; Huang, R.; Eswara, P.; Conlon, B. P., Chemical induction of aminoglycoside uptake overcomes antibiotic tolerance and resistance in Staphylococcus aureus. *Cell Chemical Biology* **2019,** *26* (10), 1355-1364. e4.
78. Allison, K. R.; Brynildsen, M. P.; Collins, J. J., Metabolite-enabled eradication of bacterial persisters by aminoglycosides. *Nature* **2011,** *473* (7346), 216-220.
79. Barraud, N.; Buson, A.; Jarolimek, W.; Rice, S. A., Mannitol enhances antibiotic sensitivity of persister bacteria in Pseudomonas aeruginosa biofilms. *PloS one* **2013,** *8* (12), e84220.
80. Cao, X.; van Putten, J. P.; Wösten, M. M., Biological functions of bacterial lysophospholipids. *Advances in Microbial Physiology* **2023,** *82*, 129-154.
81. Wright, G. C.; Weiss, J.; Kim, K. S.; Verheij, H.; Elsbach, P., Bacterial phospholipid hydrolysis enhances the destruction of Escherichia coli ingested by rabbit neutrophils. Role of cellular and extracellular phospholipases. *The Journal of clinical investigation* **1990,** *85* (6), 1925-1935.
82. de Geus, P.; van Die, I.; Bergmans, H.; Tommassen, J.; de Haas, G., Molecular cloning of pldA, the structural gene for outer membrane phospholipase of E. coli K12. *Molecular and General Genetics MGG* **1983,** *190*, 150-155.
83. Cao, X.; Brouwers, J. F.; van Dijk, L.; van de Lest, C. H.; Parker, C. T.; Huynh, S.; van Putten, J. P.; Kelly, D. J.; Wösten, M. M., The unique phospholipidome of the enteric pathogen Campylobacter jejuni: lysophosholipids are required for motility at low oxygen availability. *Journal of molecular biology* **2020,** *432* (19), 5244-5258.
84. Mouritsen, O. G., Lipids, curvature, and nano□medicine. *European journal of lipid science and technology* **2011,** *113* (10), 1174-1187.
85. Arouri, A.; Mouritsen, O. G., Membrane-perturbing effect of fatty acids and lysolipids. *Progress in lipid research* **2013,** *52* (1), 130-140.
86. Cao, X.; van de Lest, C. H.; Huang, L. Z.; van Putten, J. P.; Wösten, M. M., Campylobacter jejuni permeabilizes the host cell membrane by short chain lysophosphatidylethanolamines. *Gut Microbes* **2022,** *14* (1), 2091371.
87. Burnham, P. M.; Hendrixson, D. R., Campylobacter jejuni: collective components promoting a successful enteric lifestyle. *Nature Reviews Microbiology* **2018,** *16* (9), 551-565.
88. Campbell, E. L.; Colgan, S. P., Control and dysregulation of redox signalling in the gastrointestinal tract. *Nature Reviews Gastroenterology & Hepatology* **2019,** *16* (2), 106-120.
89. Stahl, M.; Ries, J.; Vermeulen, J.; Yang, H.; Sham, H. P.; Crowley, S. M.; Badayeva, Y.; Turvey, S. E.; Gaynor, E. C.; Li, X., A novel mouse model of Campylobacter jejuni gastroenteritis reveals key pro-inflammatory and tissue protective roles for Toll-like receptor signaling during infection. *PLoS pathogens* **2014,** *10* (7), e1004264.

90. Pan, X.; Liu, W.; Du, Q.; Zhang, H.; Han, D., Recent advances in bacterial persistence mechanisms. *International Journal of Molecular Sciences* **2023,** *24* (18), 14311.
91. Culp, E.; Wright, G. D., Bacterial proteases, untapped antimicrobial drug targets. *The Journal of antibiotics* **2017,** *70* (4), 366-377.
92. Kirsch, V. C.; Fetzer, C.; Sieber, S. A., Global inventory of ClpP-and ClpX-regulated proteins in Staphylococcus aureus. *Journal of Proteome Research* **2020,** *20* (1), 867-879.
93. Lindner, A. B.; Madden, R.; Demarez, A.; Stewart, E. J.; Taddei, F., Asymmetric segregation of protein aggregates is associated with cellular aging and rejuvenation. *Proceedings of the National Academy of Sciences* **2008,** *105* (8), 3076-3081.
94. Taylor, A. J.; Kelly, D. J., The function, biogenesis and regulation of the electron transport chains in Campylobacter jejuni: new insights into the bioenergetics of a major food-borne pathogen. *Advances in microbial physiology* **2019,** *74*, 239-329.
95. Orman, M. A.; Brynildsen, M. P., Inhibition of stationary phase respiration impairs persister formation in E. coli. *Nature communications* **2015,** *6* (1), 7983.
96. Cox, M. M., Motoring along with the bacterial RecA protein. *Nature reviews Molecular cell biology* **2007,** *8* (2), 127-138.
97. Keren, I.; Kaldalu, N.; Spoering, A.; Wang, Y.; Lewis, K., Persister cells and tolerance to antimicrobials. *FEMS microbiology letters* **2004,** *230* (1), 13-18.
98. Gutteridge, J. M.; Quinlan, G. J.; Kovacic, P., Phagomimetic action of antimicrobial agents. *Free radical research* **1998,** *28* (1), 1-14.
99. Kimura, S.; Suzuki, T., Fine-tuning of the ribosomal decoding center by conserved methyl-modifications in the Escherichia coli 16S rRNA. *Nucleic acids research* **2010,** *38* (4), 1341-1352.
100. Balaban, N. Q.; Merrin, J.; Chait, R.; Kowalik, L.; Leibler, S., Bacterial persistence as a phenotypic switch. *Science* **2004,** *305* (5690), 1622-1625.
101. Theodore, A.; Lewis, K.; Vulić, M., Tolerance of Escherichia coli to fluoroquinolone antibiotics depends on specific components of the SOS response pathway. *Genetics* **2013,** *195* (4), 1265-1276.
102. Bollen, C.; Louwagie, E.; Verstraeten, N.; Michiels, J.; Ruelens, P., Environmental, mechanistic and evolutionary landscape of antibiotic persistence. *EMBO reports* **2023,** *24* (8), e57309.

FIGURES

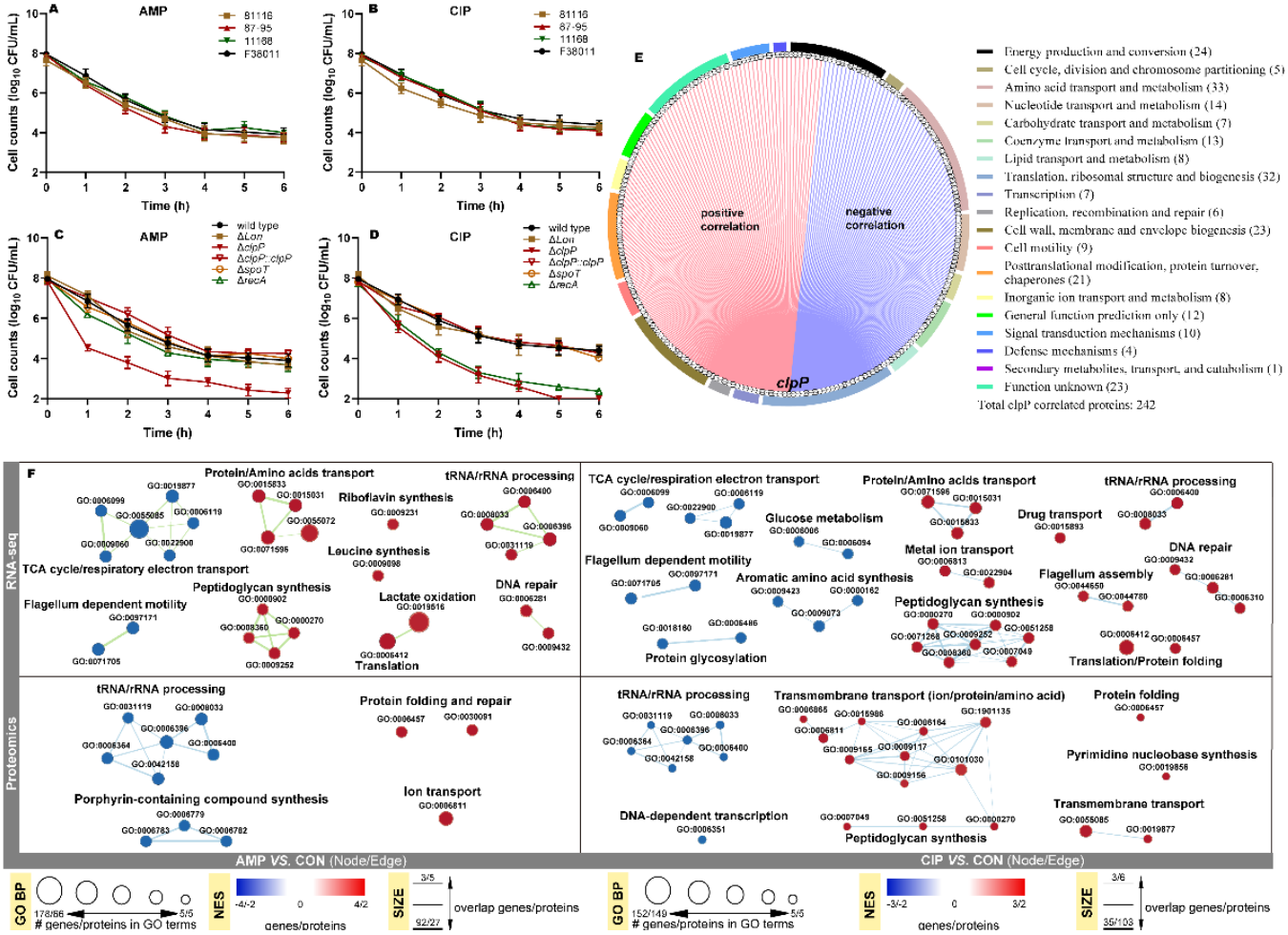

Figure 1. *clpP* is critical for *Campylobacter jejuni* persisters to tolerate ampicillin (AMP) and ciprofloxacin (CIP). (A and B) Time-killing curves of AMP and CIP against four *C. jejuni* strains, namely 81116 (dark yellow line with solid square), 87-95 (red line with solid triangle), 11168 (green line with solid inverted triangle), and F38011 (black line with solid circle). Bacterial culture of each strain was grown to optical density of 0.3 and then diluted to ~log 8 CFU/mL in MH broth with specific antibiotic at final concentration of ampicillin 100 µg/mL or ciprofloxacin 1 µg/mL. (C and D) Time-killing curves of AMP and CIP against the wild-type F38011 (black line with solid circle), Δ*lon* mutant (dark yellow line with solid square), Δ*clpP* mutant (red line with solid inverted triangle), Δ*spoT* mutant (orange line with hollow circle), Δ*recA* mutant (green line with hollow triangle), and Δ*clpP* complemented mutant Δ*clpP*::*clpP* (red line with hollow inverted triangle). (E) Cluster of orthologous groups (COG) analysis of genes strongly correlated with *clpP*. A total of 242 proteins that strongly correlated with *clpP* were identified by absolute Pearson correlation coefficients >0.8 (absolute correlation value >0.95, *p*-value <0.05). COG function analysis of the *clpP*-correlated proteins showed 19 different functional classifications, and the number of genes annotated within each classification was shown in the parenthesis. (F) Gene set enrichment analysis (GSEA) of transcriptomics and proteomics of *C. jejuni* persisters. GSEA Java (GSEA 3.0)-based graphical user interface using with a pre-ranked list of all genes or proteins based on their different expressions in antibiotic-selected persister cells and untreated cells. The cumulative distribution function was constructed by performing 1000 random gene

set membership assignments. The significantly enriched terms in transcriptome and proteome analysis were visualized in Cytoscape 3.7.1. Enrichment maps were built with stringent pathway similarity scores (Jaccard and overlap combined coefficient 0.6) and manually curated for the most representative groups of similar pathways and biological processes (GO BP). Node size corresponds to gene set size and color designates enrichment in antibiotic-selected persister cells (i.e. up-regulation after antibiotic treatment), whereas blue represents enrichment in untreated cells (i.e. down-regulation after antibiotic treatment). The thickness of lines connecting the gene-set nodes represents the degree of gene overlap between the two sets. Experiments were performed on independently grown cultures at least three times and data were presented as mean ± SD.

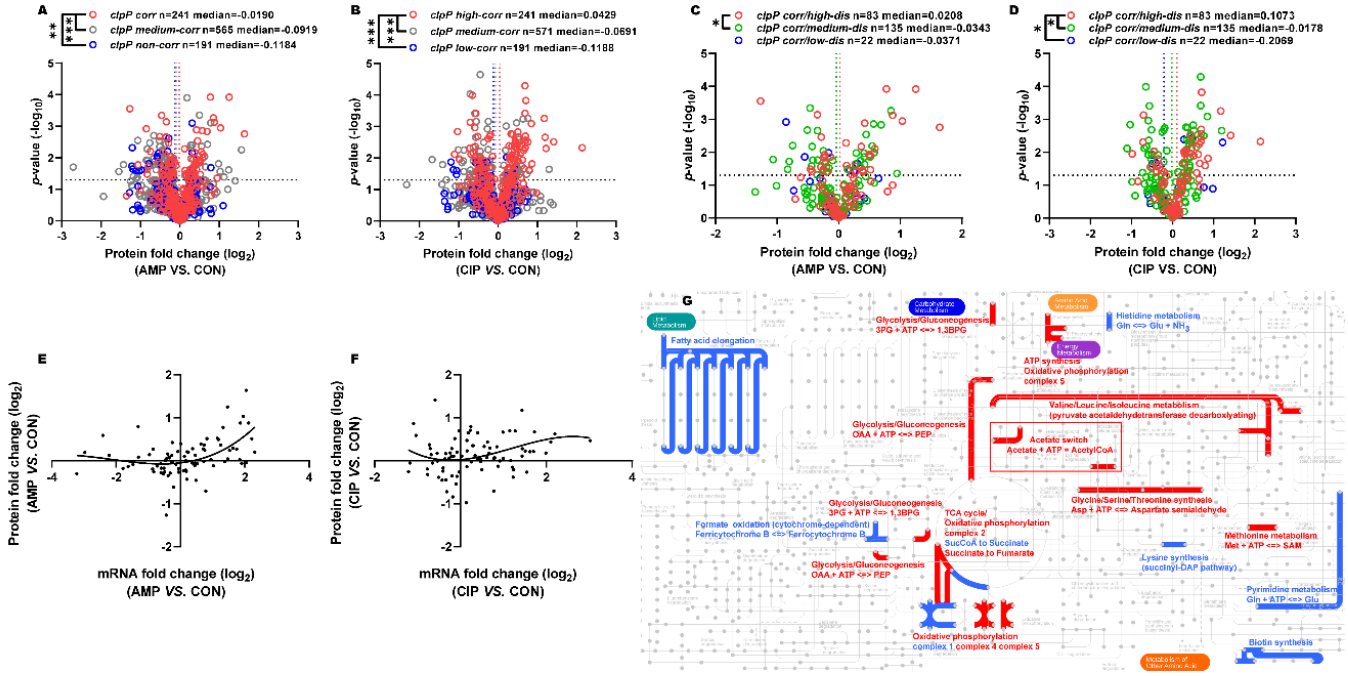

Figure 2. Metabolically active events of *C. jejuni* were *clpP*-expression dependent. (A, B, C, D) Distribution of protein abundance in *C. jejuni* F38011 persisters. Proteins were categorized into four groups based on their abundance correlation with *clpP* expression and their disorder tendency. The abundance correlation between protein and *clpP* expression was determined using Pearson's correlation coefficient analysis. Correlated features were determined as absolute coefficiency *clpP* >0.8 and *p*-value <0.05. Non-correlated features were determined as absolute coefficiency <0.2 and *p*-value <0.05. Protein disorder tendencies were predicted based on the fractions of disordered flexible linker regions in protein sequences using DFLpred. High disorder proteins were determined as disordered flexible linker residues accounting for >30% of the total sequences. Non-disorder proteins were determined as disordered flexible linker residues accounting for <10% of the total sequences. (E) Correlation analysis of *clpP* corr/high-dis features (protein-to-RNA) in *C. jejuni* F38011 persisters. (F) Gene-wise correlation of concordant changes in RNA and protein. Differentially expressed genes at the RNA level and differentially expressed proteins were compared across all pairwise comparisons. (G) Global metabolic map. Visualization of regulated biological pathway is derived from *clpP* correlated/high-disorder features. Red is denoted as promoted activity while blue is denoted as inhibited activity.

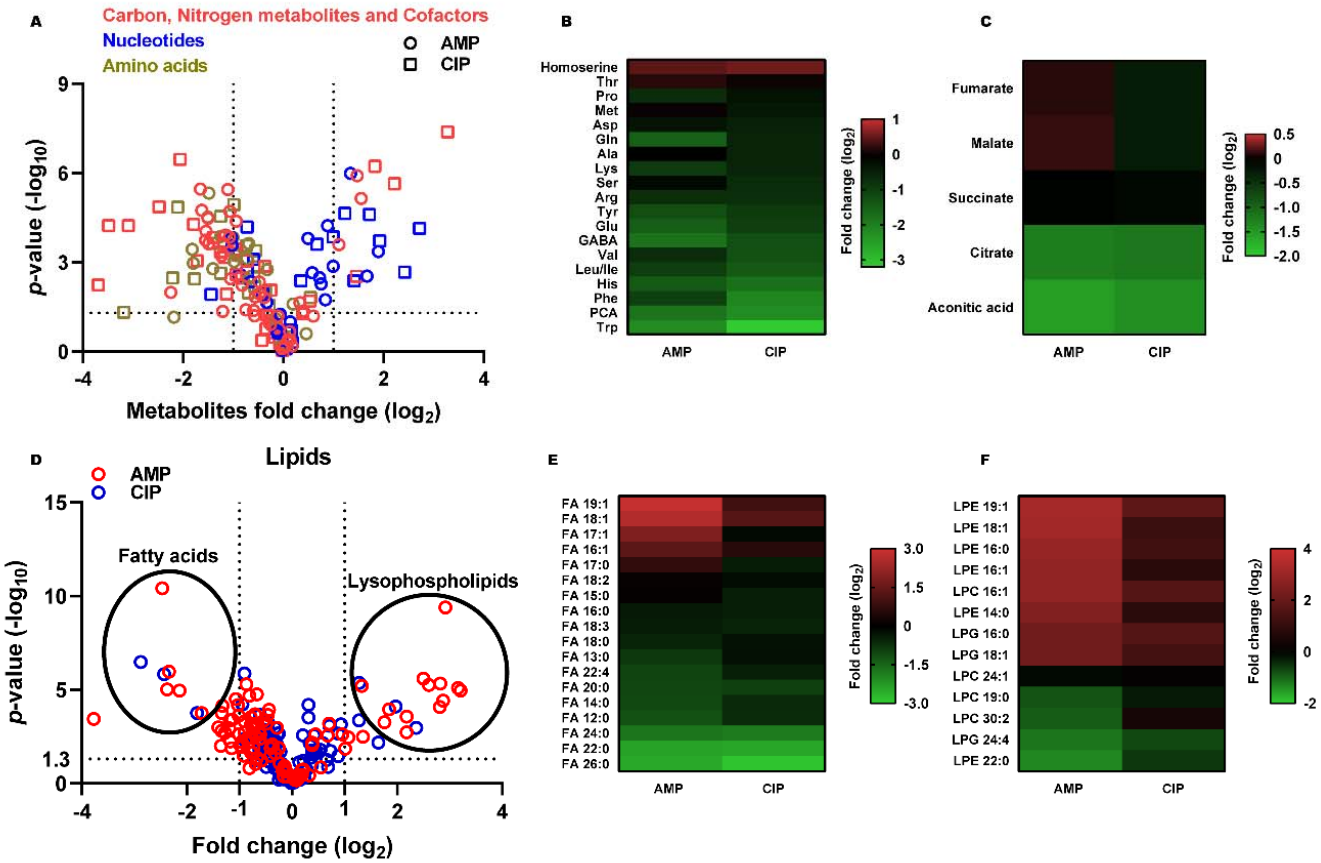

Figure 3. ***C. jejuni* F38011 persisters exhibited distinct metabolomic and lipidomic features compared to normal growing cells.** (A) Volcano plot of relative abundance change of metabolites in persister cells selected by AMP and CIP, respectively. (B) Ranked relative abundance of amino acids in persister cells. (C) Ranked relative abundance of TCA metabolites in persister cells. (D) Volcano plot of relative abundance change of lipids in persister cells selected by AMP and CIP, respectively. (E) Ranked relative abundance of fatty acids in *C. jejuni* persister cells. (F) Ranked relative abundance of lysophospholipids in *C. jejuni* persister cells.

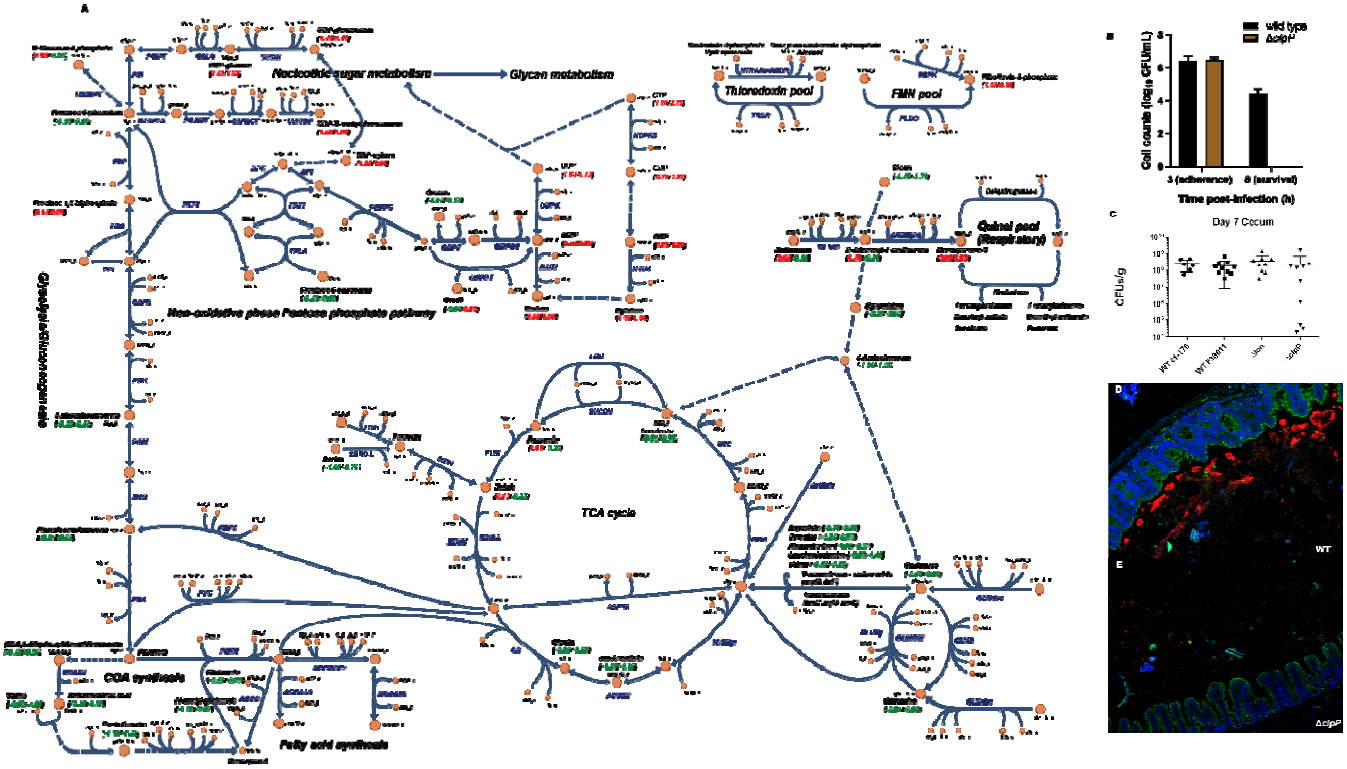

Figure 4. (A) Metabolic reprogramming of core metabolism in *C. jejuni* persister cells compared to that of normal growing cells shown as relative abundance change of metabolites (red number in parenthesis represent $\log_2$ increase and green number in parenthesis represent $\log_2$ decrease). (B, C) Survival of wild type and persistence-compromised *clpP* mutant *C. jejuni* F38011 in macrophage cells and sigirr$^{-/-}$ mice model. (D, E) Localization of wild type and persistence-compromised *clpP* mutant *C. jejuni* F38011 in the cecum of sigirr$^{-/-}$ mice.